J Fluoresc (2008) 18:329–337
DOI 10.1007/s10895-007-0272-3

ORIGINAL PAPER

Tripolyphosphate as Precursor for $REPO_4$: Eu^{3+} (RE = Y, La, Gd) by a Polymeric Method

Paulo C. de Sousa Filho · Osvaldo A. Serra

Received: 26 July 2007 / Accepted: 16 October 2007 / Published online: 10 November 2007

Abstract A modification of the Pechini method was applied to obtain luminescent rare earth orthophosphates. The developed synthetic route is based on the ability of the tripolyphosphate anion ($P_3O_{10}^{5-}$) to act both as a complexing agent and as an orthophosphate precursor. Heating of aqueous solutions containing RE^{3+}, Eu^{3+}, $P_3O_{10}^{5-}$, citric acid, and ethylene glycol led to polymeric resins. The ignition of these resins at different temperatures yielded luminescent orthophosphates. The produced nanosized phosphors (YPO_4:Eu^{3+}, (Y,Gd)PO_4:Eu^{3+}, and $LaPO_4$:Eu^{3+}) were analyzed by infrared and luminescence spectroscopies, X-ray diffractometry, and scanning electron microscopy.

Keywords Luminescence · Rare earth · Phosphates · Europium · Pechini

Introduction

The obtainment of phosphors and the improvement of their quality are widely explored themes in many branches of Chemistry, Physics, and Materials Science. Since 1896, when the first fluorescent lamp was developed by Edison, the synthesis and the improvement of inorganic luminescent materials have helped our daily lives in many ways [1]. Cathode ray tubes (CRT), X-ray detectors, projection televisions (PTV), fluorescent lamps, and plasma display panels (PDP) are some of their applications. Nowadays, properties like particle size and morphology, efficiency, luminosity, and colour purity are the main objectives of the great volume of works related to luminescent materials.

These trends were consolidated in the early 70s, when the tricolor concept was introduced with the initial aim of reproducing daylight in fluorescent lamps. This quickly led to the use of rare earth elements (RE) in luminescent materials: the employment of their unique "line-type" f-f transitions improved the phosphors colour rendering and light output considerably. The excitation and emission bands in some lanthanide ions are results of electronic transitions in the inner 4f orbitals, protected from external influences by 5s and 5p electrons. This feature leads to narrow and intense emission bands, which are applied as sources of individual colours in multiphosphor devices. So the blue (450 nm), green (545 nm), and red (610 nm) emissions of Eu^{2+}, Tb^{3+}, and Eu^{3+} have been extensively used in many commercial phosphors [1, 2].

Aiming at developing these applications, some rare earth phosphates have been studied as hosts for activator centres. For a long time, ortho-, meta-, and ultraphosphates of the rare earth elements have been the object of structural, thermal, and spectroscopic characterizations [3–8]. Their high insolubility, high chemical and physical stability, and excitation from VUV (~170 nm) to 270 nm [8] raise great interest from researches in the field of luminescent materials, mainly lamps without Hg. Nowadays, several techniques are applied for the obtainment of these materials, like colloidal synthesis [9, 10], sonochemical methods [11], spray pyrolysis [12], and high temperature solid-state reactions [8, 13].

Red phosphors are widely studied, especially those bearing the Eu^{3+} as activator. The spectroscopic behavior of this ion in different hosts has been investigated for a long

P. C. de Sousa Filho · O. A. Serra (✉)
Laboratório de Terras Raras, Departamento de Química,
Faculdade de Filosofia, Ciências e Letras de Ribeirão Preto,
Universidade de São Paulo,
Av. dos Bandeirantes, 3900,
CEP 14040-901 Ribeirão Preto, SP, Brazil
e-mail: osaserra@usp.br

time [14]. So, Eu^{3+} activated compounds, like Y_2O_3:Eu^{3+} and Y_2O_2S:Eu^{3+}, are largely employed as red emitting phosphors in many commercial appliances: their predominant emission at ~610 nm and their quantum efficiencies close to 100% make them very adequate for these applications. To be applied as a red phosphor, a material may have a high colour purity (*x* coordinate greater than 0.65), besides an acceptable quantum efficiency. For Eu^{3+}-activated compounds, this is possible when the red emissions ($^5D_0 \rightarrow {}^7F_2$ at ~610 nm) are predominant over the orange emissions ($^5D_0 \rightarrow {}^7F_1$ at ~590 nm). The spectral distribution is a consequence of the symmetry around the Eu^{3+} ions, and different host lattices lead to different spectral distributions.

This work aims at synthesiting and characterizing of Eu^{3+}-doped rare earth orthophosphates. To this end, we developed a new synthetic route using a modified polymeric method (Pechini). Modifications of the Pechini method [15] had already been successfully made by our group to obtain other europium (III)-activated compounds [16], the blue phosphor Sr_2CeO_4 [17], and Er^{3+}, Yb^{3+}-based up-converter materials [18], for example. The technique, a "chemical route," allows a homogeneous distribution of the dopant in the host and good stoichiometric control, with lower calcination temperatures than other methods. The principle of the developed synthetic route consists in the ability of the tripolyphosphate anion to act both as a complexing agent and as an orthophosphate precursor [9]. Polymeric resins were made from starting solutions containing RE nitrates, citric acid, ethylene glycol, and tripolyphosphoric acid. The ignition of these resins yield highly pure, homogeneous and nanocrystalline luminescent orthophosphates. The minimum temperature required to eliminate all impurities was ~ 650 °C; the effect of different calcination temperatures (650, 750, 850 and 950 °C) on the properties of the materials was analyzed.

Experimental

Rare earth nitrate solutions were prepared by dissolution of their oxides (Y_2O_3 99,9%—Alfa Aesar, Gd_2O_3 99,99%—Strem Chemicals, La_2O_3 99,99% and Eu_2O_3 99,99%—Rhône-Poulenc/Rhodia) in concentrated nitric acid. The pH of these solutions was found to lie between 5 and 6. Using a cation exchange resin (Dowex 50W X4 100–200 mesh), solutions of sodium tripolyphosphate (obtained from dissolution of $Na_5P_3O_{10}.6H_2O$ ~99%, purified through recrystallization from Acros-85%) were converted into tripolyphosphoric acid solutions, which were used in all synthetic processes.

For the synthesis of $REPO_4$:Eu^{3+} (RE^{3+}=Y^{3+}, $(Y_{0.83}Gd_{0.17})^{3+}$, or La^{3+}; 4% Eu^{3+}), 10.00 mL of 0.10 mol l^{-1} of $RE(NO_3)_3$ solutions and 1.00 mL of 0.04 mol l^{-1} of $Eu(NO_3)_3$ solution were mixed. Later, this solution was mixed with a tripolyphosphoric acid solution (10 mL, 0.035 mol l^{-1}), totalizing ~20 mL. The clear and colourless solution obtained as described above was stirred in a porcelain capsule for 10 min under mild heating (~50 °C) in a hot plate. Citric acid ($C_6H_8O_7$—99% Synth; 3.84 g, 20 mmol) and ethylene glycol ($C_2H_6O_2$—99.8% Aldrich; 4.8 mL, 80 mmol) were added. The resulting solution was heated up to 90–100 °C for 1 h, when a yellowish polymeric resin was formed. Still in the hot plate, the temperature was raised to ~400 °C giving rise to resin decomposition, which was completed by ignitions at different temperatures (650, 750, 850, and 950 °C) in air for 4 h. In all cases, the molar ratios for the reactants were fixed in 0.96 RE^{3+}: 0.04 Eu^{3+}: 0.33 $P_3O_{10}^{5-}$: 20 $C_6H_8O_7$: 80 $C_2H_6O_2$.

The emission and excitation spectra were recorded at room temperature on a Jobin Yvon SPEX TRIAX 550 FLUOROLOG III spectrofluorometer. By using the software apparatus, all the spectra were corrected for the lamp intensity and for the sensivity of the photomultiplier at the monitored ranges of wavelengths. The luminescence lifetime measurements were obtained using a SPEX 1934D phosphorimeter, equipped with a pulsed xenon lamp. Aiming at minimizing instrumental influences, all emission, excitation, and lifetime measurements were carried out using a filter with absorption below 500 nm at the exit (detection) of the light beam. The emission spectra were acquired with 0.2 nm emission bandpass; excitation spectra and decay curves were obtained with 1 nm emission bandpass. The values of integrated emission intensities and the exponential decay fittings for lifetimes were obtained with the use of Microcal Origin® 7.0 software. In order to evaluate the crystallinity, the materials were submitted to powder X-ray diffraction (XRD) in a SIEMENS D5005 diffractometer. The morphological analysis was carried out on a ZEISS EVO 50 scanning electron microscope (SEM). The compounds were also characterized by Fourier transform infrared spectroscopy (FTIR) on a PERKIN ELMER 502 spectrometer to elucidate their composition and structure.

Results and discussion

The FTIR spectra of all the compounds, independently of their calcination temperature, display only the characteristic bands of rare earth orthophosphates [5, 19] (Fig. 1). As expected, this indicates that there are no organic impurities in the final compositions. Moreover, the absence of characteristic bands of polyphosphates [19] confirms that the all polyphosphates were converted into orthophos-

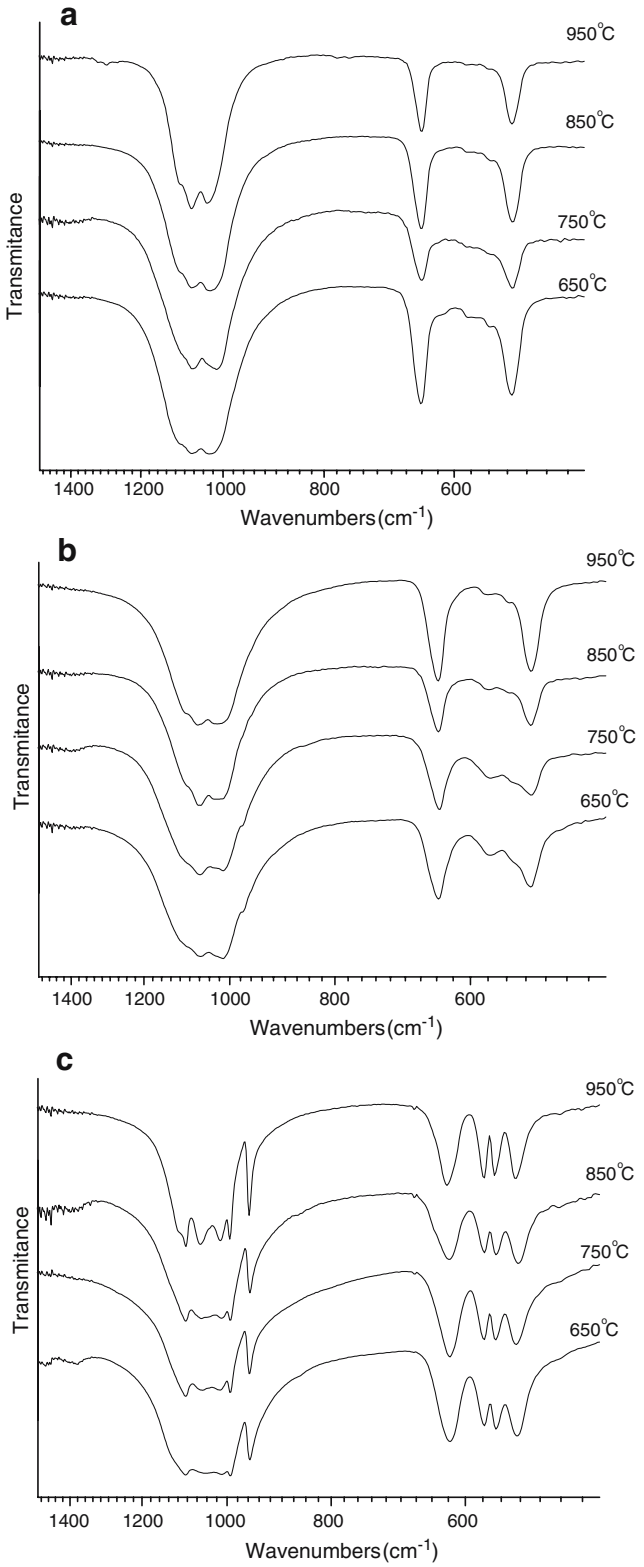

Fig. 1 Infrared spectra of phosphates preparated at different temperatures: **a** $YPO_4:Eu^{3+}$; **b** $(Y,Gd)PO_4:Eu^{3+}$; **c** $LaPO_4:Eu^{3+}$

phates. The differences between the infrared spectra are a result of different deviations from the PO_4^{3-} point group symmetry T_d to D_{2d}, D_2 and C_2 (and also more than one site symmetry), in agreement with the data reported in the literature [5].

The SEM micrographs show the morphology of the different phosphors (Fig. 2). In all compounds, there are agglomerations of 1–10 μm, and the particles are spherical,

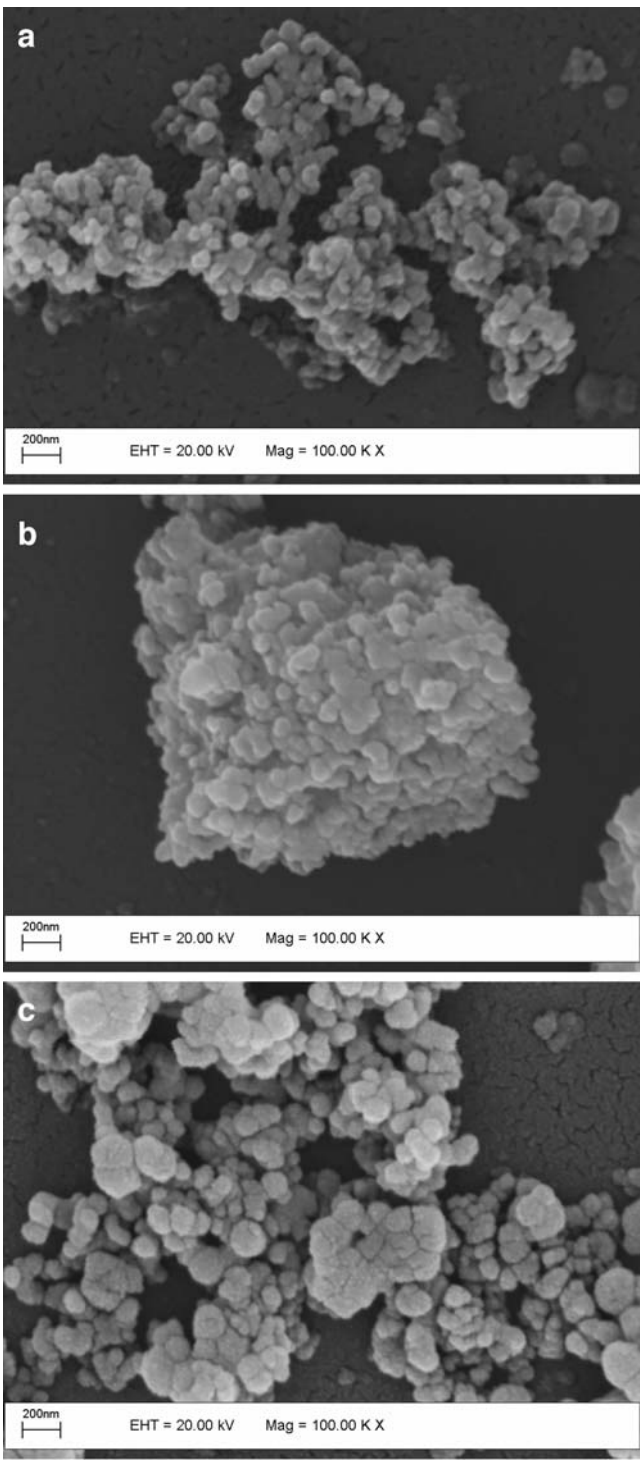

Fig. 2 Scanning electron micrographs of: **a**—$YPO_4:Eu^{3+}$ (650 °C); **b**—$(Y,Gd)PO_4:Eu^{3+}$ (650 °C); **c**—$LaPO_4:Eu^{3+}$ (950 °C) powder phosphors

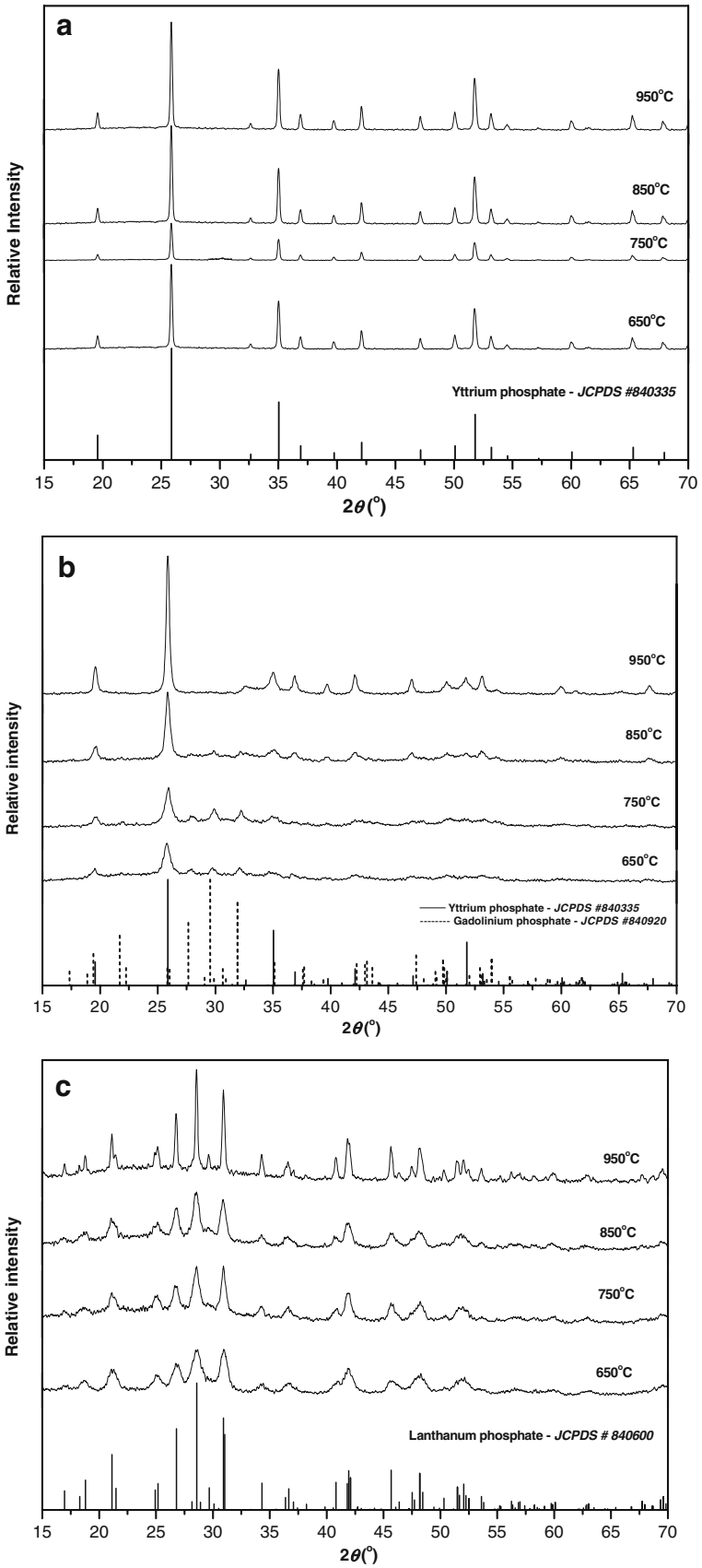

Fig. 3 X-ray diffractograms of: **a**—$YPO_4:Eu^{3+}$; **b**—$(Y,Gd)PO_4:Eu^{3+}$; **c**—$LaPO_4:Eu^{3+}$

with diameters lying between ~50 and ~200 nm. Therefore, the calcination temperature does not influence the shape of the particles. On the other hand, the particle size depends on the calcination temperature and higher temperatures cause a gathering of the particles.

The powder XRD analysis indicates good incorporation of activator centres into the host lattices and good crystalinity of the materials (Fig. 3). The diffractograms show that the phosphors diffraction patterns are in agreement with the standard YPO_4 (Zircon-Xenotime type) and $LaPO_4$ (Monazite type). The diffractogram of (Y,Gd) PO_4:Eu^{3+} differs from that of standard YPO_4 in the relative intensity of some peaks. Moreover, the presence of $GdPO_4$ main peaks denotes that the coexistence of yttrium phosphate and gadolinium phosphate (in distinct phases) is diminished at higher calcination temperatures.

By using the Scherrer method (Eq. 1), the average crystallite sizes of the phosphors were estimated by:

$$\varepsilon_{hkl} = K\lambda\left(\beta_{1/2}\right)^{-1}\cos\theta \quad (1)$$

where ε_{hkl} is the average crystallite size, K is a constant (equal to 0.89), λ is the wavelength of the X-ray ($\lambda = 1,541\ \text{Å} - Cu - K_\alpha$), $\beta_{1/2}$ is the width at half-height of the considered peak, and θ is the diffraction angle. The obtained values are shown in Table 1. All cases follow to the same trend: higher calcination temperatures lead to slightly larger crystallites.

The excitation spectra of all the compounds display the bands related to the different energy levels of Eu^{3+}, with the main band (between 393 and 395 nm) ascribed to the $^5L_6$ level (Fig. 4). The relative excitation intensity in the CTB (charge transfer band) depends on the material composition as much as on the calcination temperature (for the same composition). In the case of (Y,Gd)PO_4:Eu^{3+}, bands related to Gd^{3+} excitation at 310 nm ($^6P_{7/2}$), 304 nm ($^6P_{5/2}$), and in 274 nm (^6I_J) are also observed, which indicates that there is an energy transfer process between Gd^{3+} and Eu^{3+}.

The emission spectra of the compounds are shown in Fig. 5. In the case of YPO_4:Eu^{3+}, the predominant emission bands correspond to $^5D_0 \rightarrow {}^7F_1$ and $^5D_0 \rightarrow {}^7F_2$ transitions. An increase in the calcination temperature diminishes the difference between the emission intensities of the $^5D_0 \rightarrow {}^7F_1$ and $^5D_0 \rightarrow {}^7F_2$ bands. This indicates a little difference in the symmetry around the activator centre. The higher intensity of the hypersensitive $^5D_0 \rightarrow {}^7F_2$ transition confirms the absence of an inversion centre in the symmetry around Eu^{3+} [20, 21]. Because the $^5D_0 \rightarrow {}^7F_0$ transition is very weak, the symmetry groups D_n, D_{2d}, D_{4d}, and C_{3h} are possible for the compounds. Considering three bands for $^5D_0 \rightarrow {}^7F_1$ and four bands for $^5D_0 \rightarrow {}^7F_2$, the symmetry group D_2 can be ascribed to this phosphor [22]. If two bands were considered for $^5D_0 \rightarrow {}^7F_1$, the symmetry group D_{2d} would be more probable, which is also compatible with the Zircon-type pattern seen from the XRD analysis [3, 13, 22] and with the PO_4^{3-} infrared absorption bands [5]. This compound shows high colour purities ($0.612<x<0.650$ and $0.374<y<0.345$), which is a consequence of the narrow and intense bands of the $^5D_0 \rightarrow {}^7F_1$ and $^5D_0 \rightarrow {}^7F_2$ transitions. The high values of the x coordinate are due to the relatively intense emissions in the deep red region ($^5D_0 \rightarrow {}^7F_4$).

Table 1 Calculated crystallite sizes, $^5D_0$ luminescence lifetimes, quantum efficiencies, and chromaticity coordinates [26] of Eu^{3+}-doped rare earth phosphates

	ε_{hkl} (nm)	τ (ms)	Φ (%)	Chromatic coordinates	
				x	*y*
YPO4:Eu^{3+}					
650 °C	47	3.42	58.5	0.612	0.374
750 °C	38	3.07	45.7	0.630	0.361
850 °C	52	3.25	49.1	0.623	0.365
950 °C	57	3.47	50.7	0.650	0.345
(Y,Gd)PO4:Eu^{3+}					
650 °C	21	2.10	26.0	0.563	0.417
750 °C	21	2.15[a]	38.1	0.593	0.390
850 °C	30	2.30	23.8	0.606	0.379
950 °C	43	2.94	31.6	0.608	0.380
LaPO4:Eu^{3+}					
650 °C	15	2.44	23.1	0.613	0.376
750 °C	23	3.66	28.4	0.635	0.360
850 °C	25	3.42[a]	27.6	0.603	0.383
950 °C	69	3.60	28.5	0.591	0.395

[a] Estimated by second order decay fittings

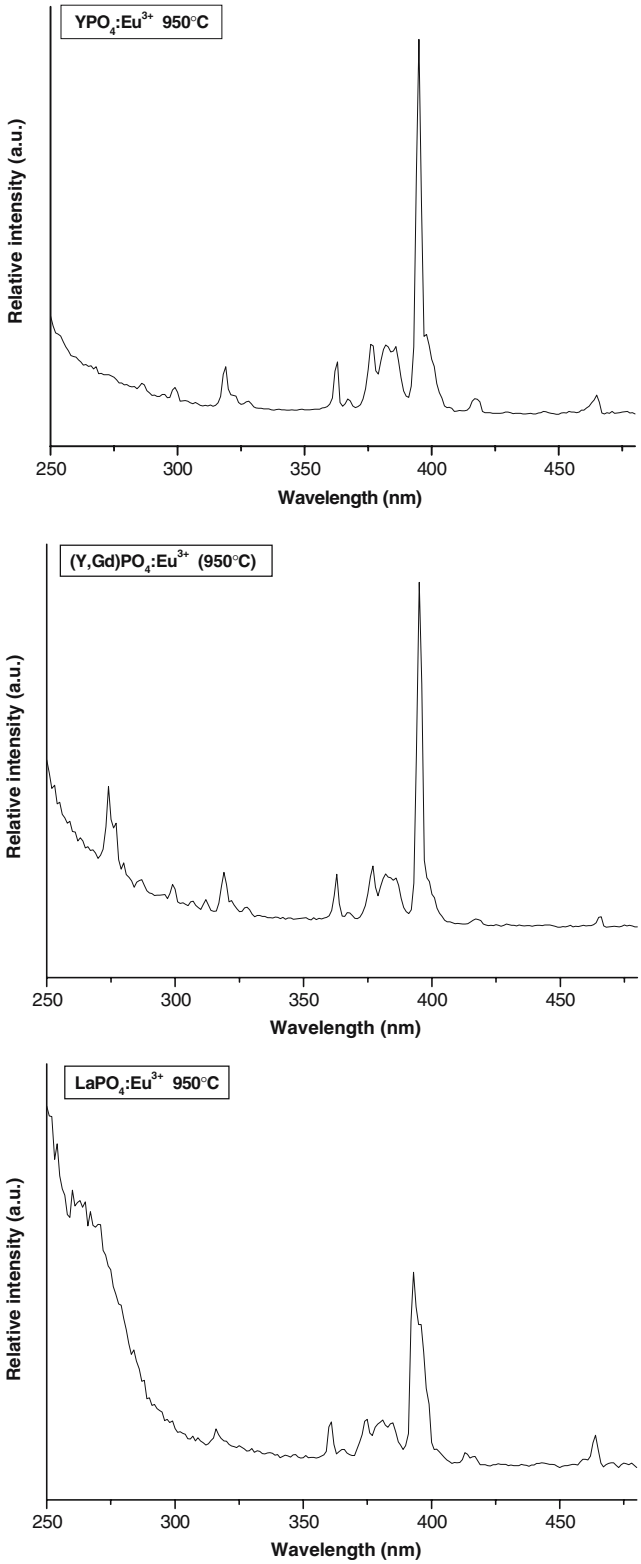

Fig. 4 Excitation spectra of $YPO_4:Eu^{3+}$ (λ_{em}=618.5 nm), $(Y,Gd)PO_4:Eu^{3+}$ (λ_{em}=618.5 nm), and $LaPO_4:Eu^{3+}$ (λ_{em}=591.0 nm)

The addition of 16% Gd^{3+} to the YPO_4 host causes small changes in the diffraction patterns of the powders, as shown in Fig. 3, and the symmetry of the compound is

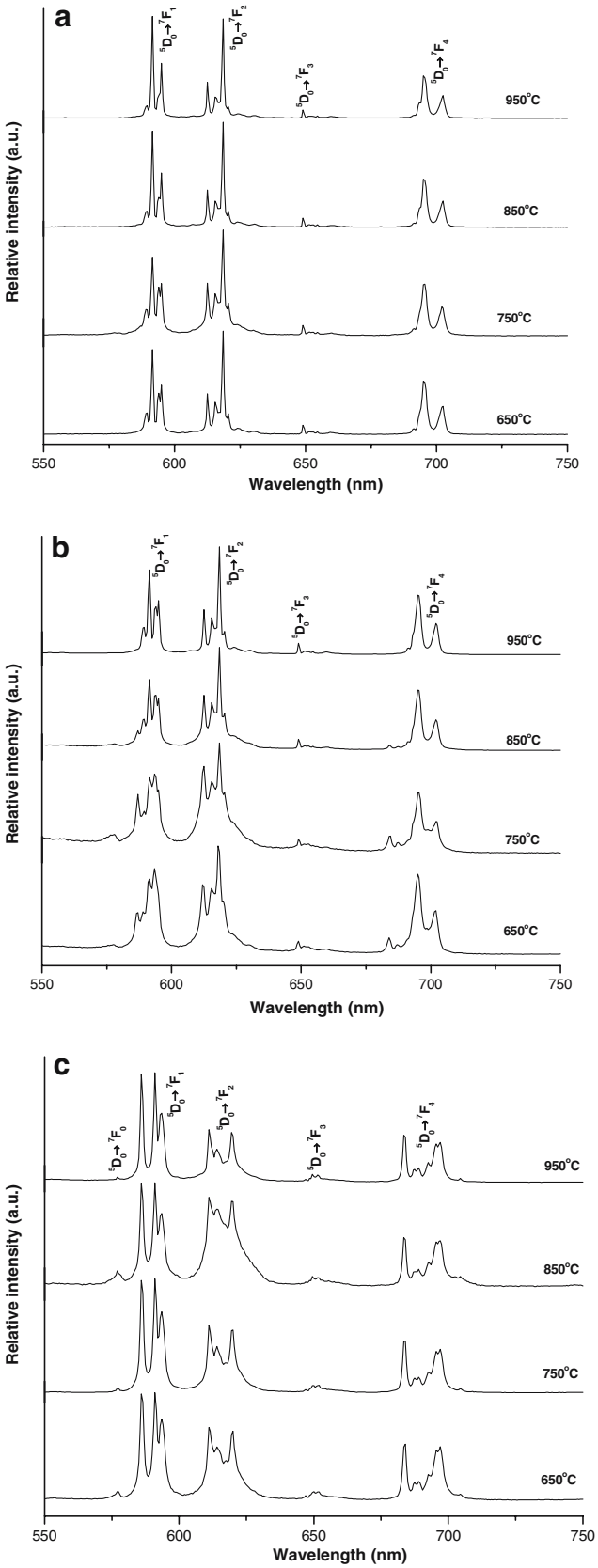

Fig. 5 Emission spectra (25 °C) of: **a**—$YPO_4:Eu^{3+}$, **b**—$(Y,Gd)PO_4:Eu^{3+}$; **c**—$LaPO_4:Eu^{3+}$ (λ_{ex}=394 nm)

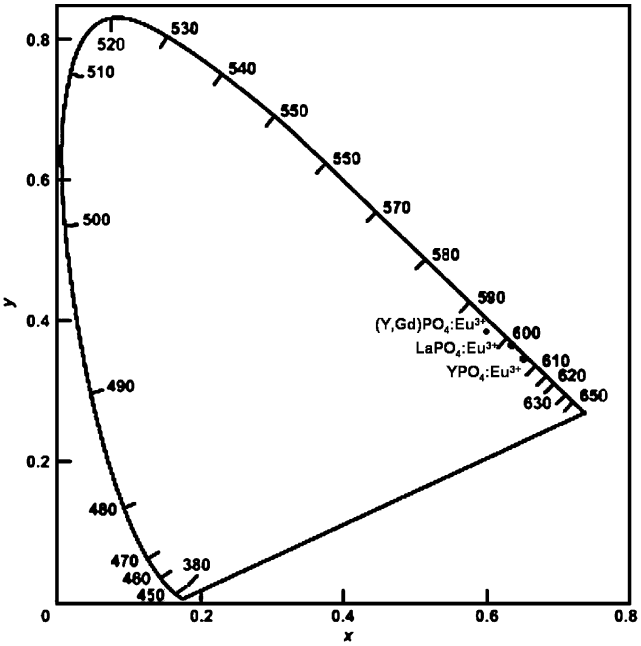

Fig. 6 Positioning of colours for the obtained "red phosphors" in the chromaticity diagram

considerably altered. The spectral distribution of the emission bands is similar to that of $YPO_4:Eu^{3+}$ (Fig. 5b). However, in the case of $(Y,Gd)PO_4:Eu^{3+}$, besides a broadening of all the emission bands, emissions relative to the $^5D_0 \rightarrow {}^7F_0$ transitions are present, and the $^5D_0 \rightarrow {}^7F_1$ and $^5D_0 \rightarrow {}^7F_4$ transitions occur with similar probabilities, presenting four or five unfoldings. This set of emissions leads to lower colour purities ($0.563<x<0.608$ and $0.417<y<0.380$) and more orange colours than those obtained for $YPO_4:Eu^{3+}$. The symmetry groups of $(Y,Gd)PO_4:Eu^{3+}$ are similar to those of $YPO_4:Eu^{3+}$. However, in the former case, the activator ion may occupy more than one symmetry site; this is indicated by the large number of unfoldings in each $^5D_0 \rightarrow {}^7F_J$ transition and by the broad $^5D_0 \rightarrow {}^7F_0$ transition [14], as well as by the presence of three or four components in the PO_4^{3-} ν_4 bands in the infrared spectra [5]. The material ignited at 950 °C shows the most resemblance with $YPO_4:Eu^{3+}$.

The emission spectra of lanthanum phosphates obtained at different temperatures display the same characteristic emission bands, with small differences in their relative intensities (Fig. 5c). In all cases, the emission spectra present one few intense and narrow band relative to the $^5D_0 \rightarrow {}^7F_0$ transition (except for 850 °C preparation), three bands relative to $^5D_0 \rightarrow {}^7F_1$ and three bands relative to $^5D_0 \rightarrow {}^7F_2$. This indicates that the Eu^{3+} ions occupy a low symmetry site (C_{2v}, C_2, C_s, C_i or C_1), being C_{2v} or C_2 symmetry groups the most probable for the compound [22]. The C_s and C_i groups, which are compatible with the Monazite-type structure [4] observed in the XRD analysis, are also possible. The predominance of the $^5D_0 \rightarrow {}^7F_1$ transition and the broad bands displayed by these compounds result in orange emission and in CIE chromaticity coordinates: $0.591<x<0.635$ and $0.360<y<0.395$, which are far from the ones required by the red standard ($x>0.65$) [23]. The chromaticity diagram shows the purest colours of the prepared compounds (Fig. 6).

Table 2 shows the relative integrated emission intensities of the $^5D_0 \rightarrow {}^7F_J$ transitions for the different host lattices. The major contribution to the red phosphors emissions arises from the $^5D_0 \rightarrow {}^7F_2$ transitions, although the $^5D_0 \rightarrow {}^7F_1$ transitions also contribute strongly for the luminescence spectra. For $YPO_4:Eu^{3+}$, the increase of the calcination temperature rises the relative importance of the $^5D_0 \rightarrow {}^7F_1$ (orange) emissions, but better colour purities are observed due to the narrowing of the emission bands. The integrated emission intensities of $YPO_4:Eu^{3+}$ also confirm that the contribution of the $^5D_0 \rightarrow {}^7F_4$ transitions, which are sensitive

Table 2 Integrated area (normalized) of the $^5D_0 \rightarrow {}^7F_J$ emissions for the prepared orthophosphates

	$^5D_0 \rightarrow {}^7F_0$	$^5D_0 \rightarrow {}^7F_1$	$^5D_0 \rightarrow {}^7F_2$	$^5D_0 \rightarrow {}^7F_3$	$^5D_0 \rightarrow {}^7F_4$
YPO4:Eu^{3+}					
650 °C	<1	81	100	9	82
750 °C	2	82	100	7	80
850 °C	<1	84	100	9	78
950 °C	<1	89	100	7	75
(Y,Gd)PO4:Eu^{3+}					
650 °C	1	74	100	7	78
750 °C	4	60	100	6	53
850 °C	2	68	100	4	42
950 °C	<1	87	100	7	71
LaPO4:Eu^{3+}					
650 °C	3	98	100	6	66
750 °C	1	100	94	8	61
850 °C	4	89	100	6	58
950 °C	1	100	79	8	58

to the Eu^{3+} environment (ΔJ=4) [21], decreases with the calcination temperature. For (Y,Gd)PO_4:Eu^{3+}, the relative integrated intensity of the $^5D_0 \rightarrow {}^7F_1$ transitions is always lower than that of integrated intensity for YPO_4:Eu^{3+}, but the same behaviour towards the increase of the calcination temperature is observed. The Eu^{3+} emissions in the monoclinic $LaPO_4$ result in very close contributions (integrated areas) for the $^5D_0 \rightarrow {}^7F_1$ and $^5D_0 \rightarrow {}^7F_2$ transitions. In this case, the $^5D_0 \rightarrow {}^7F_4$ transitions are also influenced by the ignition temperature, as observed in Table 2.

The luminescence lifetimes of the $^5D_0$ level of Eu^{3+} in different host lattices were obtained by monitoring at the maximum of the $^5D_0 \rightarrow {}^7F_1$ transition (bandwidth of ~1 nm) (Table 1). The decay curves could be fitted (except for (Y, Gd)PO_4:Eu^{3+}—750 °C, and $LaPO_4$:Eu^{3+}—850 °C), with satisfactory correlation factor, by a first order exponential decay curve; this is an indication that the activator centre occupies very similar symmetry sites [20, 21]. In the two cases mentioned above, the exponential decays were better fitted by a second order exponential decay. As already discussed, these compounds present relatively broad $^5D_0 \rightarrow {}^7F_0$ transitions, which indicates that slightly different chemical environments are occupied by Eu^{3+}. An apparent trend of the luminescence lifetimes is that higher calcination temperatures lead to longer lifetimes. The influence of the post-annealing temperature arises from the increase of the materials crystallinity at elevated ignition temperatures, which tends to cause a decrease in the rate of depopulation of the excited state by multiphonon processes [20, 21]. Moreover, there seems to be a very rough correlation between lifetimes and crystallite sizes, with larger crystallites having longer lifetimes. This suggests that the surface defects may contribute to shorten the lifetimes and, consequently, crystallites with increased surface to volume ratios (i.e. smaller radius) would relatively have more defects and corresponding shorter lifetimes. Depending on the ignition temperature and crystallite size, it is possible that even a small amount of OH groups (either adsorbed or remaining from calcinations) is present in the sample, promoting also a shortening of lifetimes.

The excited state quantum efficiencies were calculated from the emission spectra and from the luminescence lifetimes [24, 25]. The results are shown in Table 1.

Conclusion

Luminescent rare earth orthophosphates with high purity were prepared by a modified Pechini method, starting from rare earth nitrates and tripolyphosphoric acid solutions, with low ignition temperatures. The produced nanosized materials have good crystallinity and spherical morphology. The photophysical properties, as well as the medium crystallite/particle sizes, depend on the calcination temperature; larger particles are observed in higher calcination temperatures due to coalescence effects. The highest quantum efficiencies (44–58%) were found for YPO_4:Eu^{3+}; (Y, Gd)PO_4:Eu^{3+} and $LaPO_4$:Eu^{3+} have comparable quantum efficiencies (23–32%). For YPO_4:Eu^{3+} and (Y,Gd)PO_4:Eu^{3+}, the highest colour purities (x=0.650, y=0.345 and x=0.608, y=0.380 respectively) were found for calcinations at 950 °C, and for $LaPO_4$:Eu^{3+} it was found at 750 °C (x=0.635, y= 0.360).

The method is applicable for the obtainment of orthophosphates of several compositions, with a satisfactory stoichiometric control of the reactants. Moreover, besides the obtainment of luminescent powders, the technique allows the deposition of the polymeric precursors on glasses to produce orthophosphate-based thin films, both very useful for VUV excitation devices.

Acknowledgements The authors thank Dr. R.F. Silva and Dr. C.R. Neri for helpful discussions, and the Brazilian agencies CAPES, CNPq, and FAPESP for financial support.

References

1. Feldman C, Jüstel T, Ronda C, Schmidt P (2003) Inorganic luminescent materials: 100 years of research and application. Adv Funct Mater 13:511–516
2. Jüstel T, Nikol H, Ronda C (1998) New developements in the field of luminescent materials for lighting and displays. Angew Chem Int Ed 37:3084–3103
3. Hezel A, Ross SD (1967) X-ray powder data and cell dimensions of some rare earth orthophosphates. J Inorg Nucl Chem 29:2085–2089
4. Mooney RCL (1950) X-ray diffraction study of cerous phosphate and related crystals. I. Hexagonal modification. Acta Crystallogr 3:337–340
5. Kijkowska R, Cholewka E, Duszak B (2003) X-ray diffraction and Ir-absorption characteristics of lanthanide orthophosphates obtained by crystallization from phosphoric acid solution. J Mater Sci 38:223–228
6. Serra OA, Giesbrecht E (1968) Lanthanum, cerium, and praseodymium trimetaphosphates. J Inorg Nucl Chem 30:793–799
7. Gushikem Y, Giesbrecht E, Serra OA (1972) Tri- and tetrametaphosphates of lanthanidic elements. J Inorg Nucl Chem 34:2179–2187
8. Tuan DC, Olazcuaga R, Guillen F, Garcia A, Moine B, Fouassier C (2005) Luminescent properties of Eu^{3+}-doped yttrium or gadolinium phosphates. J Phys IV 123:259–263
9. Buissette V, Moreau M, Gacoin T, Boilot J-P, Chane-Ching J-Y, Le Mercier T (2004) Colloidal synthesis of luminescent rhabdophane $LaPO_4$:Ln^{3+} xH_2O (Ln=Ce, Tb, Eu; $x \approx 0.7$) nanocrystals. Chem Mater 16:3767–3773
10. Riwotzki K, Meyssamy H, Kornowski A, Haase M (2000) Liquid-phase synthesis of doped nanoparticles: colloids of luminescing $LaPO_4$:Eu and $CePO_4$:Tb particles with a narrow particle size distribution. J Phys Chem B 104:2824–2828
11. Brown SS, Im H-J, Rondinone AJ, Dai S (2005) Facile, alternative synthesis of lanthanum phosphate nanocrystals by ultrasonication. J Colloid Interface Sci 292:127–132
12. Lenggoro IW, Xia B, Mizushima H, Okuyama K, Kijima N (2001) Synthesis of $LaPO_4$:Ce,Tb phosphor particles by spray pyrolisis. Mater Lett 50:92–96

13. Serra OA, Campos RM (1991) Síntese e propriedades luminescentes de fosfatos de európio (III). Quim Nova 14(3):159–161 (in Portuguese)
14. Porcher P (1999) In: Saez R, Caro PA (eds) Rare earths–Chapter 3: Optical Properties. Editorial Complutense, Madrid
15. Pechini M (1967); U.S. Patent; 3,300,697; July 11
16. Serra OA, Cicillini SA, Ishiki RR (2000) A new procedure to obtain Eu^{3+} doped oxide and oxosalt phosphors. J Alloys Compd 303–304:316–319
17. Serra OA, Severino VP, Calefi PS, Cicillini SA (2001) The blue phosphor Sr_2CeO_4 synthesized by Pechini's method. J Alloys Compd 323–324:667–669
18. Pires AM, Heer S, Güdel HU, Serra OA (2006) Er, Yb doped yttrium based nanosized phosphors: Particle size, "host lattice" and doping ion concentration effects on upconversion efficiency. J Fluoresc 16(3):461–468
19. Corbridge DEC, Lowe J (1954) The infra-red spectra of some inorganic phosphorus compounds. J Chem Soc 493–502, http://www.rsc.org/Publishing/Journals/JR/article.asp?doi=JR9540000493
20. Blasse G, Grambmaier BC (1994) Luminescent materials. Springer-Verlag, Berlin
21. Bünzli J-CG (1989) In: Bünzli J-CG, Choppin GR (eds) Lanthanide probes in life, chemical and earth sciences–Chapter 7: Luminescent probes. Elsevier, Amsterdam
22. Forsberg JH (1973) Complexes of lanthanide (III) ions with nitrogen donor ligands. Coord Chem Rev 10:195–226
23. Wang Z, Liang H, Gong M, Su Q (2007) Luminescence investigation of Eu^{3+} activated double molybdates red phosphors with scheelite structure. J Alloys Compd 432:308–312
24. de Mello Donegá C, Alves Júnior S, de Sá GF (1997) Synthesis, luminescence and quantum yields of Eu(III) mixed complexes with 4,4,4-trifluoro-1-phenyl-1,3-butanedione and 1,10-phenanthroline-*N*-oxide. J Alloys Compd 250:422–426
25. Kodaira CA, Brito HF, Malta OL, Serra OA (2001) Luminescence and energy transfer of the europium (III) tungstate obtained via the Pechini method. J Lumin 101:11–21
26. Santa-Cruz PA, Teles FS (2003) Spectra Lux Software v.2.0, Ponto Quântico Nanodispositivos/RENAMI